Research Square

Preprints are preliminary reports that have not undergone peer review.
They should not be considered conclusive, used to inform clinical practice,
or referenced by the media as validated information.

Artery-specific prediction of percutaneous coronary intervention from coronary calcium volume on non- gated chest computed tomography

Haibo Wang
Hainan Hospital of Chinese PLA General Hospital
Fang Xu
Hainan Hospital of Chinese PLA General Hospital
Hui Lin
Hainan Hospital of Chinese PLA General Hospital
Qi Sun
Hainan Hospital of Chinese PLA General Hospital
Qinrui Xing
Hainan Hospital of Chinese PLA General Hospital
Qingnuan Fu
Hainan General Hospital
Yu Zhu
zhuyu910610@301hospital.com.cn

Hainan Hospital of Chinese PLA General Hospital

Research Article

Keywords: Non-ECG-gated chest CT, Coronary artery calcium, Three-dimensional calcium volume, Percutaneous coronary intervention, Nomogram, Artery-specific prediction

Posted Date: November 9th, 2026

DOI: https://doi.org/10.21203/rs.3.rs-11302482/v1

License: This work is licensed under a Creative Commons Attribution 4.0 International License.
Read Full License

Additional Declarations: No competing interests reported.

Title

Artery-specific prediction of percutaneous coronary intervention from coronary calcium volume on non-gated chest computed tomography

Short title: Artery-specific PCI prediction from non-gated CT

Haibo Wang [1, #], Fang Xu [1, #], Hui Lin [1, #], Qi Sun [1], Qinrui Xing [2], Qingnuan Fu [3], Yu Zhu [4, *]

[1] Department of Vascular Surgery, Hainan Hospital of Chinese PLA General Hospital, Sanya, Hainan Province, 572013, China

[2] Department of Cardiology, Hainan Hospital of Chinese PLA General Hospital, Sanya, Hainan Province, 572013, China

[3] Department of Radiology, Hainan General Hospital Branch-Ding'an Hospital, Ding'an, Hainan Province, 571200, China

[4] Department of Cardiovascular Surgery, Hainan Hospital of Chinese PLA General Hospital, Sanya, Hainan Province, 572013, China

[#] The authors worked equally.

* Corresponence: Yu Zhu (ORCID: 0000-0003-1133-8376)

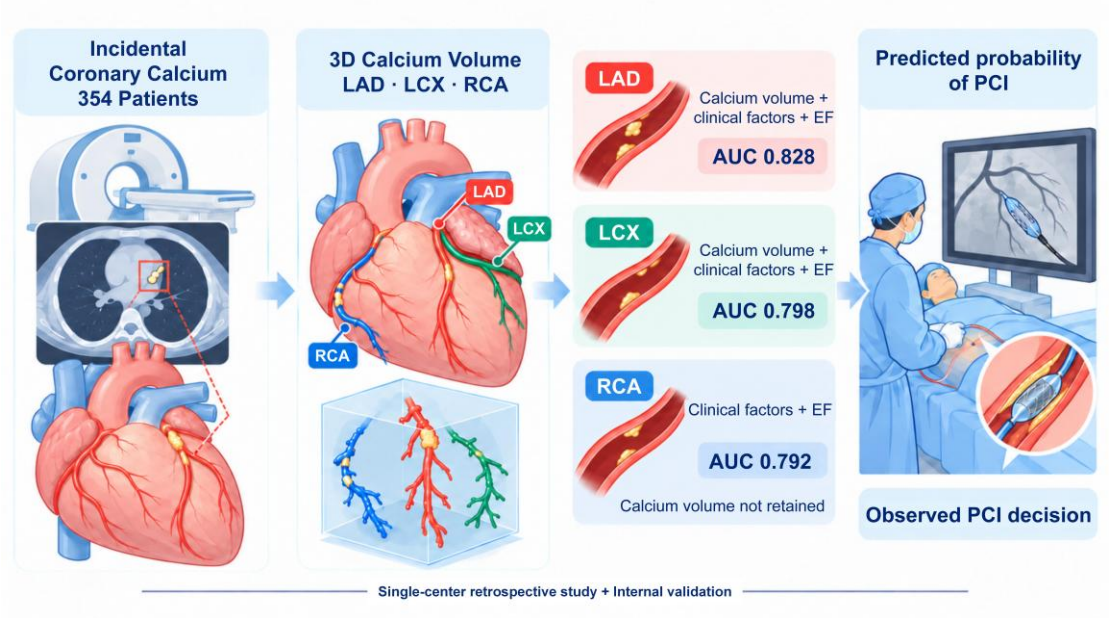
E-mail: zhuyu910610@301hospital.com.cn

Tel: +86 15692537886

Department of Cardiovascular Surgery, Hainan Hospital of Chinese PLA General Hospital, No.80 Jianglin Road, Haitang District, Sanya, Hainan Province, 572013, China.

Central Illustration

Three-dimensional coronary calcium volume was quantified from non-ECG-gated chest CT in 354 asymptomatic patients using 3D Slicer. Artery-specific PCI prediction models incorporating calcium volume, clinical factors and EF, achieved AUCs of 0.828 (LAD), 0.798 (LCX) and 0.792 (RCA). Calcium volume was not retained in the RCA model. The models may support individualized triage of incidentally detected coronary calcium. (Single-center retrospective study with internal validation.)



Abstract

Background: The clinical significance of incidental coronary calcification on non-gated chest computed tomography (CT) in asymptomatic individuals is unclear. We developed artery-specific prediction models for percutaneous coronary intervention (PCI) using three-dimensional calcium volume, with invasive angiography as the reference standard.

Methods: Calcium volume was quantified for the left anterior descending artery, left circumflex artery, and right coronary artery using 3D Slicer. Artery-specific multivariable logistic regression models were evaluated by area under the receiver operating characteristic curve (AUC), calibration, and decision curve analysis, with internal validation using 1000 bootstrap resamples.

Results: Of 354 patients, 129 (36.4%) underwent PCI. Calcium volume independently predicted PCI in the left anterior descending and left circumflex arteries but not the right coronary artery; between-artery differences were borderline and primarily driven by the right coronary artery. Ejection fraction independently predicted PCI in all models (odds ratio 0.847–0.871, all $P < 0.01$). AUCs were 0.828 (left anterior descending), 0.798 (left circumflex), and 0.792 (right coronary) arteries. Calibration was adequate for left circumflex and right coronary models; the left anterior descending model showed residual miscalibration on the Hosmer-Lemeshow test ($P = 0.008$) but acceptable agreement on bootstrap-corrected calibration. Decision curve analysis showed net benefit across a wide range of thresholds.

Conclusions: These artery-specific models may support quantitative triage of incidental coronary calcification, potentially avoiding unnecessary downstream evaluation in low-risk patients while ensuring timely revascularization in high-risk patients. Between-artery differences require confirmation in larger cohorts.

Keywords: Non-ECG-gated chest CT; Coronary artery calcium; Three-dimensional calcium volume; Percutaneous coronary intervention; Nomogram; Artery-specific prediction

Introduction

Coronary artery atherosclerotic heart disease is the leading cause of death worldwide, with an increase in morbidity and mortality rate [1]. The coronary artery calcium (CAC) score is now recognized as a useful imaging biomarker for its ability to predict major cardiovascular event risks [2]. However, a substantial proportion of individuals with detectable CAC remain asymptomatic, and their elevated calcium burden is often not incorporated into routine cardiovascular risk stratification or intervention protocols, constituting a "silent population" in clinical prevention [3, 4]. Indeed, existing risk assessment systems, largely based on conventional risk factors, provide reasonable population-level risk stratification but offer limited predictive capacity for clinically significant coronary stenosis at the individual level [5, 6].

Particularly, current available diagnostic modalities, both noninvasive and invasive all have inherent limitations. Exercise electrocardiography and myocardial perfusion imaging are insensitive to early, hemodynamically non-significant plaques and carry non-negligible false-positive and false-negative rates [7]. Invasive coronary angiography, despite being the anatomical gold standard, is unsuitable for widespread screening due to its invasive nature and high cost. Coronary computed tomography angiography, although possessing excellent negative predictive value, is constrained by contrast agent requirements, heart rate control, electrocardiographic gating dependence, and limited accessibility, rendering it impractical for population-based screening in asymptomatic individuals [8].

In recent years, opportunistic use of non-ECG-gated chest computed tomography (CT) has garnered increasing attention. With the widespread adoption of low-dose CT for lung cancer screening and the growing use of preoperative chest imaging, the volume of non-ECG-gated chest CT examinations has increased substantially. These examinations, originally intended for pulmonary or mediastinal evaluation, simultaneously depict coronary artery calcium burden without additional radiation exposure or contrast agent administration. Prior studies have demonstrated that calcium scores derived from non-ECG-gated chest CT correlate strongly with those derived from ECG-gated coronary CT angiography and carry consistent prognostic value, positioning non-ECG-gated chest CT as a natural platform for opportunistic cardiovascular screening [2].

Nevertheless, for patients without overt coronary symptoms in whom CAC is incidentally detected on non-ECG-gated chest CT obtained for health screening or non-cardiac indications, optimal management remains unclear and lacks consensus. CAC scoring has been incorporated into the framework for lipid-lowering goal setting, with higher scores triggering more intensive therapeutic targets. Guidelines indicated that CAC detected on non-ECG-gated chest CT should be reported and used to guide cardiovascular risk factor assessment and primary prevention decisions, rather than serving as a routine indication for further imaging or cardiology referral

[2, 9].

Despite guideline recommendations against triaging incidental calcium to downstream testing, many non-cardiologists, lacking quantifiable and actionable risk stratification tools, nonetheless refer such patients for coronary CT angiography or invasive angiography. Some patients without significant stenosis incur added costs and radiation exposure, and their primary care may be delayed. Others with high calcific burden may have significant stenosis that goes unrecognized. Guidelines specify that CAC should guide lipid therapy but offer no threshold to determine when further coronary evaluation is warranted. Clinicians lack evidence-based tools to support individualized triage decisions [2, 10].

Recent studies have demonstrated the feasibility of deep learning-based automated CAC scoring on non-ECG-gated chest CT, yet the literature to date has largely focused on concordance with ECG-gated measurements or on long-term event prediction [11]. Few studies have directly addressed the clinical decision point at issue to predict the presence of significant stenosis requiring percutaneous coronary intervention in asymptomatic and non-cardiac populations, thereby enabling individualized triage for downstream coronary evaluation. Moreover, most prior investigations have relied on the Agatston score, a density-weighted semi-quantitative metric influenced by slice thickness and scanner characteristics, whereas three-dimensional calcium volume may more faithfully reflect calcific burden [12]. The open-source imaging platform 3D Slicer offers an auditable and generalizable means of precisely extracting artery-specific calcium volumes.

The present study used 3D Slicer to quantify CAC volumes from non-ECG-gated chest CT in asymptomatic patients with incidental findings, using invasive coronary angiography as the reference standard. We integrated calcium volumes with clinical, laboratory and electrocardiographic data to build a nomogram predicting significant stenosis requiring PCI, with internal validation and decision curve analysis. The goal is to provide a quantitative triage tool, based on existing imaging data without additional cost or radiation, to spare low-risk patients from unnecessary coronary evaluation while ensuring high-risk patients receive timely cardiology referral and revascularization.

Methods

Ethical statement

This study is a single center retrospective study following the ethical principles of the declaration of Helsinki. The study protocol was reviewed and approved by the medical ethics committee of Hainan Hospital of Chinese PLA General Hospital (approval No. S2026-36-01). The requirement for informed consent was waived, given that the retrospective nature of the study and the use of anonymous clinical data.

Study population

Patients were consecutively enrolled from our single center between January 2025 and December 2025. All patients underwent non-gated chest CT with imaging reports indicating high-density calcification along the course of the coronary arteries. Inclusion criteria were: (1) absence of overt coronary symptoms at presentation; patients with typical exertional angina, acute coronary syndrome, or heart failure symptoms were excluded. Non-specific or atypical chest discomfort, when recorded during routine history taking, did not constitute an exclusion criterion and was analyzed as a clinical variable; (2) non-gated chest CT performed for health screening or non-cardiac indications (e.g., pulmonary nodules or preoperative evaluation); (3) invasive coronary angiography performed within 1 month after CT examination. Exclusion criteria were: (1) history of coronary heart disease or confirmed acute/chronic myocardial infarction; (2) presence of intracardiac metal implants (coronary stents, pacemakers, prosthetic valves); (3) prior coronary artery bypass grafting; (4) severe aortic root or valvular calcification interfering with CAC interpretation; (5) severe motion artifacts on CT images precluding reliable calcification analysis; (6) poor angiographic image quality precluding accurate stenosis assessment; (7) calcification involving the left main coronary artery.

The following data were collected: (1) baseline demographic and clinical characteristics; (2) CT imaging parameters and quantitative calcification data; (3) coronary angiography findings; (4) laboratory tests, electrocardiography, echocardiography, and other ancillary test results.

CT image acquisition

All patients underwent non-ECG-gated chest CT without intravenous contrast administration, heart rate control, or electrocardiographic gating. Images were acquired using a 256-detector row CT scanner (Revolution CT, GE Healthcare, Milwaukee, WI, USA). Images were acquired at 120 kVp with automatic tube current modulation, a 512 × 512 matrix, and a slice thickness of 1.25 mm. The scan range extended from the lung apex to the diaphragm, covering the entire thorax and heart. All images were reconstructed with a soft tissue kernel.

Volume quantification of coronary artery calcification based on 3D slicer

Coronary artery calcified lesions were defined as plaque foci with intraluminal attenuation greater than 130 Hounsfield units (HU) within the territories of the three major coronary arteries: the left circumflex artery (LCX), right coronary artery (RCA), and left anterior descending artery (LAD) [13, 14]. Semi-automated segmentation was performed using 3D Slicer (version 5.12) to extract the calcification volume of each artery, which were recorded as LCX calcification volume, LAD calcification volume, and RCA calcification volume, respectively. Calcification volumes were measured by two experienced clinicians independently; each reader performed three replicate measurements and the per-reader mean was used, with discrepancies resolved by consensus. Inter-observer agreement assessed by the intraclass correlation

coefficient was 0.982 (CI: 0.980-0.984, $P < 0.001$).

Invasive coronary angiography

All patients underwent selective coronary angiography with the standard Judkins technique. Two experienced interventional cardiologists independently assessed the percent diameter stenosis of each artery. Significant stenosis was defined as luminal diameter stenosis ≥70%, or ≥50% for the left main coronary artery. The decision to perform percutaneous coronary intervention was recorded based on the angiographic findings.

Clinical data collection

The following data were collected through the electronic medical record system: (1) demographic characteristics: age, gender, height, weight (BMI), heart rate, systolic blood pressure, diastolic blood pressure; (2) Cardiovascular risk factors: history of hypertension, diabetes, hyperlipidemia, smoking, drinking, family history of coronary heart disease, history of peripheral arterial disease, history of heart failure, and history of atrial fibrillation; (3) Laboratory indicators: white blood cell count, red blood cell count, hemoglobin, platelet count, prothrombin time, thrombin time, fibrinogen, activated partial thromboplastin time, D-dimer, triglyceride, total cholesterol, high density lipoprotein, low density lipoprotein, alanine aminotransferase, aspartate aminotransferase, creatinine, estimated glomerular filtration rate; (4) ECG: abnormal ST segment and T wave; (5) Echocardiography: abnormal left ventricular ejection fraction and wall motion.

Outcome definition

The primary outcome was the decision to perform PCI during the index admission, as recorded in the catheterization report; the decision was made by the interventional cardiology team and was not protocolized. Angiographic significance was defined separately as ≥70% diameter stenosis of at least one major epicardial artery or ≥50% for the left main coronary artery. The models therefore predict the clinical decision to perform PCI, which is closely related to but not identical with angiographic stenosis severity. Twelve patients with isolated left main disease were classified in the non-PCI group.

Statistical analysis

Statistical analyses were performed using R software (version 4.3.0; R Foundation for Statistical Computing, Vienna, Austria) and SPSS 26.0 (IBM Corp., Armonk, NY, USA). The proportion of missing data was <3% for all continuous variables and missing values were imputed using the median. Categorical variables had no missing data and were analyzed using complete-case analysis. Continuous variables following a normal distribution are presented as mean ± SD; non-normally distributed variables are presented as median (Q1, Q3). Categorical variables are presented as counts (percentages). Patients were stratified according to whether

PCI was performed. Intergroup comparisons were performed using the independent-samples t-test for normally distributed continuous variables, the Mann-Whitney U test for non-normally distributed continuous variables, and the χ^2 test or Fisher's exact test for categorical variables, as appropriate. Spearman's rank correlation coefficient was used to assess the correlation between coronary artery calcium volume and corresponding angiographic stenosis severity. The primary outcome was the performance of PCI. Variable selection was performed using least absolute shrinkage and selection operator (LASSO) regression, with the optimal λ value determined via 10-fold cross-validation. Variables selected by LASSO were subsequently entered into a multivariable logistic regression model. Stepwise forward selection was used to identify independent predictors. Adjusted odds ratios (ORs) with 95% CIs were calculated for each independent factor. Based on the final multivariable logistic regression model, a nomogram was constructed using the rms package in R software. Each predictor was assigned a weighted score according to its regression coefficient, and the total score corresponded to the predicted probability of undergoing PCI. Model discrimination was assessed using the area under the receiver operating characteristic curve (AUC), with optimism-corrected C-index calculated via 1000 bootstrap resamples. Calibration was evaluated using calibration plots and the Hosmer-Lemeshow goodness-of-fit test ($P > 0.05$ indicating adequate fit). Decision curve analysis was performed to evaluate the clinical net benefit across a range of threshold probabilities. For the between-artery comparison, data were reshaped into a long format with one record per patient per artery. A mixed-effects logistic regression model and, as a sensitivity analysis, generalized estimating equations (GEE) with robust variance were fitted, both including a calcium volume × artery interaction term, with calcium volume standardized (per +1 SD) and adjusted for 10 shared clinical variables. The estimated working correlation for GEE was approximately zero, and results were identical across exchangeable, independence, and AR1 structures. These analyses were performed post hoc and should be considered exploratory. All statistical tests were two-sided and $P < 0.05$ was considered statistically significant.

Results

Baseline characteristics

A total of 354 patients were included in the final analysis, of whom 129 (36.4%) underwent PCI and 225 (63.6%) did not (Figure 1). The baseline characteristics are summarized in Table 1. The mean age was 63.34 ± 10.23 years, and 208 patients (58.76%) were male. Compared with the non-PCI group, patients in the PCI group had a significantly higher prevalence of diabetes (37.21% vs 26.22%, $P = 0.041$) and chest pain (60.47% vs 46.22%, $P = 0.014$), and a significantly lower prevalence of hyperlipidemia (13.18% vs 23.11%, $P = 0.033$) and HDL-C level [1.05 (0.91, 1.18) vs 1.13 (0.95, 1.33) mmol/L, $P = 0.003$]. No significant differences were observed between the two groups in age, sex, BMI, hypertension, smoking history,

drinking history, family history of coronary heart disease, heart rate, blood pressure, or other laboratory parameters including blood cell counts, coagulation indices, lipid profiles, liver enzymes, and renal function (all $P > 0.05$).

Electrocardiographic and echocardiographic findings differed significantly between groups. The PCI group had a higher proportion of wall motion abnormalities (28.68% vs 3.56%, $P < 0.001$) and a lower left ventricular ejection fraction (57.71% ± 5.51% vs 63.32% ± 4.82%, $P < 0.001$). The prevalence of ST-segment abnormality was numerically higher in the PCI group but did not reach statistical significance (21.71% vs 14.22%, $P = 0.097$). No significant difference was found in T-wave abnormality between the two groups ($P = 0.512$).

Coronary calcium volume and angiographic stenosis severity

Representative examples of coronary calcium segmentation using 3D Slicer are shown in Figure 2. The distribution of coronary calcium volume and angiographic stenosis severity stratified by PCI status is presented in Table 2. Patients who underwent PCI had significantly higher total calcium volume [229.91 (45.92, 523.44) mm^3 vs 98.76 (6.07, 352.33) mm^3, $P < 0.001$], LAD calcium volume [146.98 (23.53, 351.76) mm^3 vs 55.95 (0, 243.47) mm^3, $P < 0.001$], LCX calcium volume [294 (0, 781.73) mm^3 vs 0 (0, 30.83) mm^3, $P = 0.015$], and RCA calcium volume [11.73 (0, 53.84) mm^3 vs 0 (0, 37.56) mm^3, $P = 0.004$] compared with the non-PCI group.

Angiographic stenosis severity was consistently higher in the PCI group across all three coronary arteries: LAD [85% (70%, 95%) vs 40% (10%, 50%), $P < 0.001$], LCX [50% (0, 90%) vs 0 (0, 40%), $P < 0.001$], and RCA [60% (40%, 90%) vs 20% (0, 50%), $P < 0.001$].

Correlation analysis showed that calcium volume was weakly correlated with the corresponding angiographic stenosis severity (LAD: $R^2 = 0.084$; LCX: $R^2 = 0.031$; RCA: $R^2 = 0.038$; all $P < 0.001$). Despite the statistical significance, calcium volume explained less than 10% of the variance in stenosis severity, indicating that stenosis severity cannot be predicted by calcium volume alone (Figure 3).

Multivariable logistic regression analyses

Artery-specific PCI was performed in 102 patients for the LAD (28.8%), 54 for the LCX (15.3%) and 65 for the RCA (18.4%); 129 patients underwent PCI overall, indicating multi-artery intervention in a proportion of patients. The results of univariable and multivariable logistic regression analyses for predictors of PCI in each coronary artery are presented in Table 3.

LAD model. In the multivariable analysis, peripheral arterial disease (OR = 5.374, 95% CI: 1.192–24.231, $P = 0.029$), chest pain (OR = 2.153, 95% CI: 1.236–3.749, $P = 0.007$), wall motion abnormality (OR = 3.430, 95% CI: 1.545–7.617, $P = 0.002$), ejection fraction (OR =

0.847, 95% CI: 0.797–0.901, $P < 0.001$), and LAD calcium volume (OR = 1.002, 95% CI: 1.001–1.002, $P = 0.002$) were independently associated with LAD-PCI.

LCX model. Diabetes (OR = 2.633, 95% CI: 1.364–5.082, P = 0.004), chest pain (OR = 2.422, 95% CI: 1.222–4.803, $P = 0.011$), ST-segment abnormality (OR = 3.112, 95% CI: 1.448–6.507, $P = 0.003$), ejection fraction (OR = 0.871, 95% CI: 0.824–0.920, $P < 0.001$), and LCX calcium volume (OR = 1.001, 95% CI: 1.000–1.002, $P = 0.035$) were independently associated with LCX-PCI.

RCA model. BMI (OR = 1.090, 95% CI: 1.005–1.184, $P = 0.039$), hypertension (OR = 2.212, 95% CI: 1.147–4.266, $P = 0.018$), peripheral arterial disease (OR = 7.483, 95% CI: 1.704–32.863, $P = 0.007$), and ejection fraction (OR = 0.859, 95% CI: 0.814–0.906, $P < 0.001$) were independently associated with RCA-PCI. Notably, RCA calcium volume did not enter the final multivariable model (OR = 1.000, 95% CI: 0.999–1.001, $P = 0.877$).

Artery-specific predictors and between-artery differences

Calcium volume was independently associated with PCI in the LAD and LCX, whereas no significant association was observed in the RCA. Because calcium volume was modelled on its native scale and its distribution differed substantially between arteries (median LAD 81.30 mm^3, LCX 0.00 mm^3, RCA 1.59 mm^3, with marked zero-inflation in the LCX and RCA), odds ratios expressed per mm^3 are not directly comparable across models. To formally test for between-artery differences, data were reshaped into a long format and two complementary models were fitted: a mixed-effects logistic regression model with patient ID as a random intercept, and generalized estimating equations (GEE) with robust variance as a sensitivity analysis. Both models included a calcium volume × artery interaction term, with calcium volume standardized (per +1 SD) and adjustment for 10 shared clinical variables. The estimated working correlation for GEE was approximately zero, and results were identical across exchangeable, independence, and AR1 structures. The two methods yielded consistent qualitative findings but differed in the strength of evidence. With mixed-effects modelling, the RCA vs LAD/LCX interaction was statistically significant (P = 0.022 after adjustment), whereas with GEE, the corresponding contrast was of borderline significance (P = 0.051 after adjustment). In both models, the LAD vs LCX interaction was not significant (P = 0.083 and P = 0.692, respectively). The adjusted odds ratios per +1 SD increase were 1.47/1.42 for the LAD, 1.47/1.31 for the LCX, and 0.93/1.02 for the RCA (mixed-effects/GEE). These findings indicate that the between-artery heterogeneity was primarily driven by the RCA, which differed from the LAD and LCX territories, whereas the LAD and LCX did not differ. The evidence should be regarded as borderline and model-dependent, and requires confirmation in larger cohorts.

In contrast, ejection fraction was consistently and independently associated with PCI across all three artery-specific models (LAD: OR = 0.847, $P < 0.001$; LCX: OR = 0.871, $P < 0.001$; RCA:

OR = 0.859, $P = 0.006$), underscoring the universal role of left ventricular systolic function in driving revascularization decisions regardless of the target artery. Chest pain was a significant predictor in both the LAD and LCX models but not in the RCA model, whereas diabetes and ST-segment abnormality were significant only in the LCX model, and peripheral arterial disease was significant in both the LAD and RCA models.

Nomogram construction

Based on the independent predictors identified in the artery-specific multivariable logistic regression models, artery-specific nomograms were constructed to estimate the probability of requiring PCI in each coronary artery (Figure 4). For the LAD model, the nomogram incorporated peripheral arterial disease, chest pain, wall motion abnormality, ejection fraction, and LAD calcium volume (Figure 4A). For the LCX model, diabetes, chest pain, ST-segment abnormality, ejection fraction, and LCX calcium volume were included (Figure 4B). For the RCA model, BMI, hypertension, peripheral arterial disease, and ejection fraction were included (Figure 4C).

To facilitate clinical application, an online dynamic nomogram was developed and is accessible at https://zhuyu.shinyapps.io/pci-predictor/ (Figure 5A). An example is provided for predicting the probability of PCI intervention for a patient with EF = 60% and LAD calcium volume = 1000 mm^3. A quick response code linking to the online dynamic nomogram is provided in Figure 5B.

Model validation and predictive performance

The LAD model achieved the highest discriminative ability, with an AUC of 0.828 (95% CI: 0.780–0.876), followed by the LCX model (AUC = 0.798, 95% CI: 0.734–0.862) and the RCA model (AUC = 0.792, 95% CI: 0.734–0.849) (Figure 6A). Bootstrap internal validation with 1000 resamples yielded optimism-corrected C-indices of 0.816, 0.778, and 0.777 for the LAD, LCX, and RCA models, respectively.

Calibration curves demonstrated good agreement between predicted probabilities and observed outcomes for all three models (Figure 6B–6D). The Hosmer-Lemeshow test P values were 0.008, 0.423, and 0.155 for the LAD, LCX, and RCA models, respectively. Calibration was adequate for the LCX and RCA models, whereas the LAD model showed evidence of miscalibration ($P = 0.008$); however, the bootstrap-corrected calibration curve, together with a calibration slope of 1.098, an intercept of 0.081, and a Brier score of 0.151, indicated reasonable overall agreement.

Decision curve analysis showed that all three models provided net clinical benefit over a wide range of threshold probabilities compared with the "treat all" and "treat none" strategies (Figure 6E). The LAD model exhibited the highest net benefit across the clinically relevant threshold

range (0.2–0.4), consistent with its superior discriminative performance.

Sensitivity analysis

Several sensitivity analyses were performed to evaluate the robustness of the primary findings. First, calcification volume was analyzed as a dichotomous variable (presence vs. absence of calcification) within each artery-specific model. The presence of calcification was independently associated with PCI in all three territories: LAD (OR = 2.20, 95% CI: 1.04–4.64, $P = 0.039$), LCX (OR = 2.08, 95% CI: 1.06–4.06, $P = 0.032$) and RCA (OR = 2.19, 95% CI: 1.17–4.08, $P = 0.014$). Second, among patients with measurable calcification, tertiles of calcification volume were analyzed. A graded increase in the rate of PCI was observed across tertiles in the LAD territory (19.6%, 35.9% and 41.3%; highest vs. lowest tertile: OR = 2.92, 95% CI: 1.33–6.41, $P = 0.008$); a similar, although non-significant, trend was observed for the LCX territory (16.1%, 20.0% and 27.3%; OR = 1.76, 95% CI: 0.61–5.07, $P = 0.293$), whereas no dose–response relationship was found for the RCA territory (OR = 0.77, 95% CI: 0.29–2.08, $P = 0.610$). Third, when calcification volume was retained as a continuous variable (per 100 mm^3 increase), the results were consistent with the primary analyses for the LAD (OR = 1.16, 95% CI: 1.05–1.28, $P = 0.003$) and LCX (OR = 1.12, 95% CI: 1.01–1.25, $P = 0.034$) territories, whereas RCA calcification volume was not associated with PCI (OR = 0.99, 95% CI: 0.89–1.11, $P = 0.877$). Taken together, these analyses support the robustness of the artery-specific models and indicate that the association between calcification volume and PCI is territory-specific.

Discussion

In this study, we extracted three-dimensional coronary calcium volume from non-ECG-gated chest CT and constructed artery-specific prediction models for PCI in the left anterior descending artery (LAD), left circumflex artery (LCX) and right coronary artery (RCA), using invasive coronary angiography as the reference standard.

Artery-specific differences in the predictive effect of calcium volume

We observed artery-specific differences in the association between calcium volume and the PCI decision. Between-artery comparison using mixed-effects and GEE models suggested that the heterogeneity was primarily driven by the RCA (P = 0.022–0.051 after adjustment), whereas the LAD and LCX did not differ (P = 0.083–0.692). This difference parallels the relative myocardial supply territories: the LAD supplies approximately 70% of left ventricular myocardial mass, whereas the RCA predominantly supplies the right ventricle, which is more tolerant to ischemia. These anatomical differences may underlie the weaker association between RCA calcium volume and RCA-PCI. Our study extended previous observations by formally demonstrating that the predictive effect of calcium volume differs between the RCA and the LAD/LCX territories, although this evidence was borderline and model-dependent.

A previous study demonstrated that CCTA-derived morphologic parameters had higher predictive performance for hemodynamically significant stenosis in the LAD than in the LCX or RCA [15]. The reliability of non-ECG-gated CT calcium scoring varied across institutions, suggesting that both scanner-related and artery-specific factors may influence the stability of calcium quantification and the strength of its clinical association [16]. Our study extended these observations by using PCI decision as the endpoint and formally demonstrating that the predictive effect of calcium volume differs between the RCA and the LAD/LCX territories, thereby providing an artery-level basis for risk stratification when interpreting incidentally detected coronary calcium on non-ECG-gated chest CT.

Why RCA calcium volume did not enter the final model

The absence of RCA calcium volume from the final RCA-PCI model warranted interpretation from both statistical and biological perspectives. Statistically, the number of RCA-PCI events may have been lower than that of LAD-PCI, resulting in insufficient statistical power and a potential false-negative finding. Furthermore, the median RCA calcium volume in the non-PCI group was 0 (0, 37.56), indicating that a substantial proportion of patients had low RCA calcium burden. This skewed distribution may have compromised the stability of effect estimation. Biologically, the RCA supplied a relatively smaller myocardial territory, and the right ventricle is more tolerant to ischemia. These may lead clinicians to adopt a higher intervention threshold for RCA lesions compared with LAD lesions.

Notably, the final RCA model incorporated BMI, hypertension, peripheral arterial disease and ejection fraction. These factors were all systemic clinical factors rather than local calcium metrics. This finding suggested that RCA-PCI decisions may be driven more by the patient's overall cardiovascular risk profile and cardiac functional status than by local calcium burden alone [17].

An alternative explanation is that the effect of RCA calcium volume may be mediated by variables retained in the final model. RCA calcium burden may contribute to global left ventricular dysfunction, which is captured by ejection fraction, and hypertension and peripheral arterial disease may reflect systemic atherosclerotic burden encompassing RCA disease. The effect of RCA calcium volume may therefore be partially or fully mediated rather than directly predictive, warranting formal mediation analysis in future studies.

In addition, RCA-PCI decisions may rely more on symptoms and electrocardiographic findings than on local calcium burden. Inferior ischemia often presents atypically, potentially leading clinicians to base intervention decisions on overall risk assessment rather than on RCA calcium volume alone. This pattern may differ from LAD lesions, where calcium burden itself often drives the decision.

Ejection fraction as a cross-artery common predictor

Left ventricular ejection fraction independently predicted PCI in all three artery-specific models. Regardless of which artery harbors the calcific burden, left ventricular systolic function served as a common driver of PCI decision-making. Reduced ejection fraction suggested hemodynamically significant stenosis with consequent impairment of left ventricular performance. Irrespective of the culprit artery, clinicians are inclined to pursue revascularization to improve myocardial perfusion and cardiac function.

A previous study found that adding clinical and functional parameters to CCTA-derived morphologic indices significantly improved the prediction of hemodynamically significant stenosis [15]. Our study further demonstrated that ejection fraction retains stable independent predictive value across artery-specific models. This suggested that when coronary calcium is incidentally detected on non-ECG-gated chest CT, comprehensive risk assessment should incorporate left ventricular functional evaluation by echocardiography.

Clinical implications of artery-specific predictor combinations

The final predictor combinations differed substantially across the three artery-specific models. The LAD model incorporated peripheral arterial disease, chest pain, wall motion abnormality, ejection fraction, and LAD calcium volume, encompassing symptomatic, functional, and calcific dimensions. The LCX model incorporated diabetes, chest pain, ST-segment abnormality, ejection fraction, and LCX calcium volume, adding metabolic and electrocardiographic indices to the LAD model framework. The RCA model was dominated by BMI, hypertension, peripheral arterial disease, and ejection fraction, with calcium volume failing to enter the final model.

These differences reflected the heterogeneity in pathophysiological characteristics and clinical decision-making patterns across different coronary supply territories. These findings suggested that incidentally detected coronary calcium on non-ECG-gated chest CT should not be treated equivalently across arteries. LAD calcium warranted heightened attention and proactive evaluation. LCX calcium should be interpreted in conjunction with metabolic and electrocardiographic indices, whereas RCA calcium should be managed primarily through systemic risk assessment.

Clinically, the three artery-specific models can be applied by calculating the predicted probability of PCI for each artery and using the highest probability as an indicator of overall risk. In cases of discordant results, the highest-risk artery should guide the decision. The online dynamic nomogram facilitates rapid computation at the point of care.

Model calibration and validation

The LCX and RCA models demonstrated adequate calibration (Hosmer-Lemeshow test P = 0.423 and P = 0.155, respectively), with good agreement between predicted and observed

probabilities. However, the LAD model showed a statistically significant Hosmer-Lemeshow result ($\chi^2 = 20.78$, $df = 8$, $P = 0.008$), suggesting potential miscalibration.

It should be noted that the Hosmer-Lemeshow test is highly sensitive to sample size and dependent on the arbitrary grouping of predicted probabilities. Therefore, it should not be used as the sole metric for assessing calibration. Other calibration metrics should be considered in conjunction: the LAD model had a calibration slope of 1.098, an intercept of 0.081, and a Brier score of 0.151. The bootstrap-corrected calibration curve also indicated acceptable agreement between predicted and observed probabilities, with preserved discrimination. Nevertheless, the possibility of miscalibration in the LAD model should not be dismissed, and a statistically significant Hosmer-Lemeshow result should prompt caution in interpreting predicted probabilities, particularly in the intermediate-to-high risk range. The wide spectrum of LAD calcification burden, with relatively few observations in the intermediate-to-high risk range, may have contributed to the instability of the calibration curve. In addition, the decision to perform PCI was influenced by multiple unmeasured determinants, including plaque composition, physiological assessment, and operator judgement. External validation with recalibration, if necessary, is warranted before clinical implementation.

Limitations

This work had several limitations. First, it was a single-center retrospective study with a limited sample size (354 patients). The relatively low number of RCA-PCI events may have resulted in insufficient statistical power and the absence of RCA calcium volume from the final model requires validation in larger cohorts. Second, PCI decision-making was influenced by physician judgment, patient preference and healthcare policy, and is not solely determined by anatomical stenosis severity. Selection bias may therefore be present. Third, the LAD model showed a Hosmer-Lemeshow P value of 0.008, indicating potential miscalibration. Although other calibration metrics suggested acceptable overall agreement, further evaluation and recalibration in external validation are warranted. Fourth, external validation was not performed and the generalizability of the models warrants confirmation in multi-center datasets. Last, the between-artery comparison was performed post hoc and should be considered exploratory. The evidence for the RCA vs LAD/LCX difference was borderline and model-dependent. The LAD–LCX comparison was underpowered, and the absence of a significant difference should not be interpreted as evidence of equivalence. The zero-inflated distribution of LCX and RCA calcium volumes (53% and 48% zero values) warrants cautious interpretation.

Conclusions

We extracted three-dimensional coronary calcium volume from non-ECG-gated chest CT and constructed artery-specific prediction models for PCI. Between-artery comparison suggested that the predictive effect of calcium volume differed primarily between the RCA and the

LAD/LCX territories. Left ventricular ejection fraction independently predicted PCI in all three models. The predictor combinations differed across artery-specific models, reflecting the heterogeneity in pathophysiological characteristics and clinical decision-making patterns across coronary supply territories. This work provides an artery-specific risk stratification tool based on existing imaging data without additional examination or radiation, for asymptomatic patients with incidentally detected coronary calcium on non-ECG-gated chest CT. This work potentially enabled low-risk patients to avoid unnecessary coronary evaluation while ensuring high-risk patients receive timely specialist assessment and revascularization.

Clinical trial number: Not applicable.

Acknowledgement

The authors would like to thank the 3D Slicer development team and the open-source community for making this powerful and freely available image analysis platform accessible to researchers worldwide. Without their sustained dedication to open-source software development, the quantitative calcium volume analysis in this study would not have been possible.

CRediT authorship contribution statement

Haibo Wang: Conceptualization, Methodology, Investigation, Formal analysis, Funding acquisition, Writing – original draft. **Fang Xu**: Conceptualization, Methodology, Validation, Investigation, Writing – original draft. **Hui Lin**: Methodology, Software, Data curation, Formal analysis, Writing – original draft. **Qi Sun**: Investigation, Resources, Data curation. **Qinrui Xing**: Investigation, Resources. **Qingnuan Fu**: Investigation, Resources. **Yu Zhu**: Conceptualization, Supervision, Project administration, Funding acquisition, Validation, Writing – review & editing. All authors have read and approved the final manuscript.

Funding sources

This work was supported by the Nanhai New Star projects for Science and Technology Innovation Talent (NHXXKJCX202532), Nanhai New Star projects for Medicine and Health Talent, Hainan Provincial Natural Science Foundation of China (824QN405) and Beijing Natural Science Foundation-Daxing Innovation Joint Fund (Cultivation Project) (L256068).

Data availability

The data underlying this article will be shared on reasonable request to the corresponding author.

Declarations Conflict of interest

The authors declare that they have no known competing financial interests or personal relationships that could have appeared to influence the work reported in this paper.

References

1. van der Bijl P, Gulati M, Saraste A, Marwick T, Kwong R, Blankstein R, Nieman K, Sengupta PP, van Rosendael A, Knuuti J *et al*: Contemporary, non-invasive imaging diagnosis of chronic coronary artery disease. *Lancet* 2025, 406(10519):2577-2587.
2. Foraker R, Sperling L, Bratzke L, Budoff M, Leppert M, Razavi AC, Rodriguez F, Shapiro MD, Whelton S, Wong ND *et al*: Opportunistic Detection of Coronary Artery Calcium on Noncardiac Chest Computed Tomography: An Emerging Tool for Cardiovascular Disease Prevention: A Scientific Statement From the American Heart Association. *Circulation* 2025, 152(19):e391-e401.
3. Sun KJ, Whelton SP, Feldman L, Johnson PT, Azadi JR: Things We Do for No Reason™: Overlooking incidental coronary artery calcification (iCAC). *J Hosp Med* 2025, 20(12):1351-1354.
4. Hagopian R, Strebel T, Bernatz S, Myers GA, Offerman E, Zuniga E, Kim CY, Ng AT, Iwaz JA, Nürnberg L *et al*: AI Opportunistic Coronary Calcium Screening at Veterans Affairs Hospitals. *Nejm ai* 2025, 2(6).
5. Anderson JL, Le VT, Min DB, Biswas S, Minder CM, McCubrey RO, Knight S, Horne BD, Mason S, Lappe DL *et al*: Comparison of Three Atherosclerotic Cardiovascular Disease Risk Scores With and Without Coronary Calcium for Predicting Revascularization and Major Adverse Coronary Events in Symptomatic Patients Undergoing Positron Emission Tomography-Stress Testing. *Am J Cardiol* 2020, 125(3):341-348.
6. Osborne-Grinter M, Ali A, Williams MC: Prevalence and clinical implications of coronary artery calcium scoring on non-gated thoracic computed tomography: a systematic review and meta-analysis. *Eur Radiol* 2024, 34(7):4459-4474.
7. Mirshahvalad SA, Chavoshi M, Hekmat S: Diagnostic performance of prone-only myocardial perfusion imaging versus coronary angiography in the detection of coronary artery disease: A systematic review and meta-analysis. *J Nucl Cardiol* 2022, 29(3):1339-1351.
8. Narula J, Chandrashekhar Y, Ahmadi A, Abbara S, Berman DS, Blankstein R, Leipsic J, Newby D, Nicol ED, Nieman K *et al*: SCCT 2021 Expert Consensus Document on Coronary Computed Tomographic Angiography: A Report of the Society of Cardiovascular Computed Tomography. *J Cardiovasc Comput Tomogr* 2021, 15(3):192-217.
9. Hecht HS, Cronin P, Blaha MJ, Budoff MJ, Kazerooni EA, Narula J, Yankelevitz D, Abbara S: 2016 SCCT/STR guidelines for coronary artery calcium scoring of noncontrast noncardiac chest CT scans: A report of the Society of Cardiovascular Computed Tomography and Society of Thoracic Radiology. *J Cardiovasc Comput Tomogr* 2017, 11(1):74-84.
10. Vrints C, Andreotti F, Koskinas KC, Rossello X, Adamo M, Ainslie J, Banning AP, Budaj A, Buechel RR, Chiariello GA *et al*: 2024 ESC Guidelines for the management of chronic coronary syndromes. *Eur Heart J* 2024, 45(36):3415-3537.
11. Choi JH, Cha MJ, Cho I, Kim WD, Ha Y, Choi H, Lee SH, You SC, Chang JS: Validation of deep learning-based fully automated coronary artery calcium scoring using non-ECG-gated chest CT in patients with cancer. *Front Oncol* 2022, 12:989250.

12. Chen Y, Hu Z, Li M, Jia Y, He T, Liu Z, Wei D, Yu Y: Comparison of Nongated Chest CT and Dedicated Calcium Scoring CT for Coronary Calcium Quantification Using a 256-Dector Row CT Scanner. *Acad Radiol* 2019, 26(10):e267-e274.
13. Devia-Rodriguez R, Derksen M, de Groot K, Vedder IR, Zeebregts CJ, Bokkers RPH, Pol RA, de Vries JPM, Schuurmann RCL: Validation of a Length-Adjusted Abdominal Arterial Calcium Score Method for Contrast-Enhanced CT Scans. *Diagnostics (Basel)* 2023, 13(11).
14. Holcombe SA, Horbal SR, Ross BE, Brown E, Derstine BA, Wang SC: Variation in aorta attenuation in contrast-enhanced CT and its implications for calcification thresholds. *PLoS One* 2022, 17(11):e0277111.
15. Wang C, Leng S, Tan RS, Chai P, Fam JM, Teo LLS, Chin CY, Ong CC, Baskaran L, Keng YJF *et al*: Coronary CT Angiography-based Morphologic Index for Predicting Hemodynamically Significant Coronary Stenosis. *Radiol Cardiothorac Imaging* 2023, 5(6):e230064.
16. Suh YJ, Kim C, Lee JG, Oh H, Kang H, Kim YH, Yang DH: Fully automatic coronary calcium scoring in non-ECG-gated low-dose chest CT: comparison with ECG-gated cardiac CT. *Eur Radiol* 2023, 33(2):1254-1265.
17. Chen C, Chen M, Tao Q, Hu S, Hu C: Non-contrast CT-based radiomics nomogram of pericoronary adipose tissue for predicting haemodynamically significant coronary stenosis in patients with type 2 diabetes. *BMC Med Imaging* 2023, 23(1):99.

Table 1. Baseline characteristics of the study population.

Covariate	Total Patients (n=354)	Non-PCI Group (n=225)	PCI Group (n=129)	*P* value
Age, years	63.34±10.23	63.19±10.12	63.59±10.46	0.728
Gender, Male n (%)	208 (58.76%)	128 (56.89%)	80 (62.02%)	0.406
BMI, kg/m^2	25.07±3.42	25.02±3.59	25.17±3.13	0.691
Hypertension, n (%)	218 (61.58%)	135 (60.00%)	83 (64.34%)	0.487
Diabetes, n (%)	107 (30.23%)	59 (26.22%)	48 (37.21%)	0.041
Hyperlipidemia, n (%)	69 (19.49%)	52 (23.11%)	17 (13.18%)	0.033
Peripheral arterial disease, n (%)	8 (2.26%)	3 (1.33%)	5 (3.88%)	0.146
Heart failure history, n (%)	3 (0.85%)	2 (0.89%)	1 (0.78%)	1.000
Atrial fibrillation history, n (%)	14 (3.95%)	11 (4.89%)	3 (2.33%)	0.364
Stroke, n (%)	54 (15.25%)	30 (13.33%)	24 (18.60%)	0.184
Chest pain, n (%)	182 (51.41%)	104 (46.22%)	78 (60.47%)	0.014
Smoking history, n (%)	131 (37.01%)	81 (31.00%)	50 (38.76%)	0.687
Drinking history, n (%)	146 (41.24%)	84 (41.78%)	52 (40.31%)	0.875
Family history of coronary heart disease, n (%)	6 (1.69%)	4 (1.78%)	2 (1.55%)	1.000
Heart rate, bpm	78.43±11.87	78.03±11.63	79.12±12.31	0.411
Systolic pressure, mmHg	131.75±17.14	130.91±16.64	133.22±17.95	0.232
Diastolic pressure, mmHg	75.41±11.74	75.32±11.67	75.57±11.91	0.843
White blood cell, $x10^9/L$	6.49 (5.38, 7.85)	6.48 (5.34, 7.76)	6.50 (5.59, 7.89)	0.548
Red blood cell, $x10^{12}/L$	4.50±0.60	4.51±0.63	4.48±0.56	0.661
Hemoglobin, g/L	134.60±16.18	134.76±15.85	134.33±16.81	0.815
Platelet, $x10^9/L$	213 (188.00, 250.75)	213.00 (189.11, 249.00)	213.00 (189.00, 249.00)	0.904
Prothrombin time, s	10.70 (10.30, 11.17)	10.70 (10.30, 11.10)	10.80 (10.30, 11.20)	0.663
Thrombin time, s	14.66±1.11	14.71±1.06	14.57±1.18	0.268
Activated partial thrombin time, s	30.66±3.31	30.62±3.51	30.46±2.94	0.735
Fibrinogen, g/L	3.14 (2.79, 3.56)	3.14 (2.81, 3.54)	3.18 (2.79, 3.62)	0.619

D-dimer, mg/L	0.33 (0.21, 0.48)	0.33 (0.22, 0.48)	0.31 (0.20, 0.46)	0.637
Triglyceride, mmol/L	1.35 (1.03, 1.98)	1.30 (1.02, 1.98)	1.46 (1.07, 1.92)	0.220
Total cholesterol, mmol/L	4.12 (3.55, 4.72)	4.12 (3.45, 4.69)	4.01 (3.62, 4.72)	0.801
LDL-C, mmol/L	2.35±0.89	2.35±0.91	2.37±0.86	0.856
HDL-C, mmol/L	1.10 (0.94, 1.29)	1.13 (0.95, 1.33)	1.05 (0.91, 1.18)	0.003
Alanine Aminotransferase, U/L	18.55 (13.25, 25.58)	18.60 (13.80, 24.40)	18.50 (12.70, 26.30)	0.752
Aspartate Aminotransferase, U/L	18.30 (15.00, 22.10)	18.50 (14.90, 22.20)	18.10 (15.10, 21.60)	0.904
Creatinine, umol/L	76.00 (64.30, 88.60)	75.00 (63.95, 87.60)	76.60 (64.50, 89.50)	0.602
eGFR, (mL/min/1.73m^2)	83.36±18.33	83.09±17.16	83.82±20.26	0.729
ST segment abnormality, n (%)	60 (16.95%)	32 (14.22%)	28 (21.71%)	0.097
T wave abnormality, n (%)	128 (36.16%)	78 (34.67%)	50 (38.76%)	0.512
Wall motion abnormality, n (%)	45 (12.71%)	8 (3.56%)	37 (28.68%)	<0.001
EF, %	61.28±5.75	63.32±4.82	57.71±5.51	<0.001

Values are mean ± SD or median (interquartile range) for continuous variables and n (%) for categorical variables. PCI, percutaneous coronary intervention; BMI, body mass index; EF, ejection fraction; eGFR, estimated glomerular filtration rate.

Table 2. Coronary calcium volume and angiographic stenosis severity stratified by PCI status.

Covariate	**Total Patients (n=354)**	**Non-PCI Group (n=225)**	**PCI Group (n=129)**	***P* value**
Calcification volume, mm^3				
Total volume	142.71 (18.33, 416.69)	98.76 (6.07, 352.33)	229.91 (45.92, 523.44)	<0.001
LAD	81.30 (5.56, 298.73)	55.95 (0, 243.47)	146.98 (23.53, 351.76)	<0.001
LCX	0 (0, 44.63)	0 (0, 30.83)	294 (0, 781.73)	0.015
RCA	1.59 (0, 44.85)	0 (0, 37.56)	11.73 (0, 53.84)	0.004
Stenosis severity, %				
LAD	50% (30%, 80%)	40% (10%, 50%)	85% (70%, 95%)	<0.001
LCX	20% (0, 50%)	0 (0, 40%)	50% (0, 90%)	<0.001
RCA	40% (0, 60%)	20% (0, 50%)	60% (40%, 90%)	<0.001

Values are median (Q1, Q3). PCI, percutaneous coronary intervention; LAD, left anterior descending artery; LCX, left circumflex artery; RCA, right coronary artery.

Table 3. Multivariable logistic regression analyses of factors associated with PCI intervention in different coronary arteries.

Coronary arteries	Variable	OR	95% CI		*P* value
LAD	Peripheral arterial disease	5.374	1.192	24.231	0.029
	Chest pain	2.153	1.236	3.749	0.007
	Wall motion abnormality	3.430	1.545	7.617	0.002
	Ejection fraction	0.847	0.797	0.901	<0.001
	LAD calcification volume	1.002	1.001	1.002	0.002
LCX	Diabetes	2.633	1.364	5.082	0.004
	Chest pain	2.422	1.222	4.803	0.011
	ST segment abnormality	3.112	1.448	6.507	0.003
	Ejection fraction	0.871	0.824	0.920	<0.001
	LCX calcification volume	1.001	1.000	1.002	0.035
RCA	BMI	1.090	1.005	1.184	0.039
	Hypertension	2.212	1.147	4.266	0.018
	Peripheral arterial disease	7.483	1.704	32.863	<0.001
	Ejection fraction	0.859	0.814	0.906	0.006

OR, odds ratio; CI, confidence interval; BMI, body mass index; LAD, left anterior descending artery; LCX, left circumflex artery; RCA, right coronary artery.

Figures and Legends

Figure 1. Flow Diagram of Participant Selection.

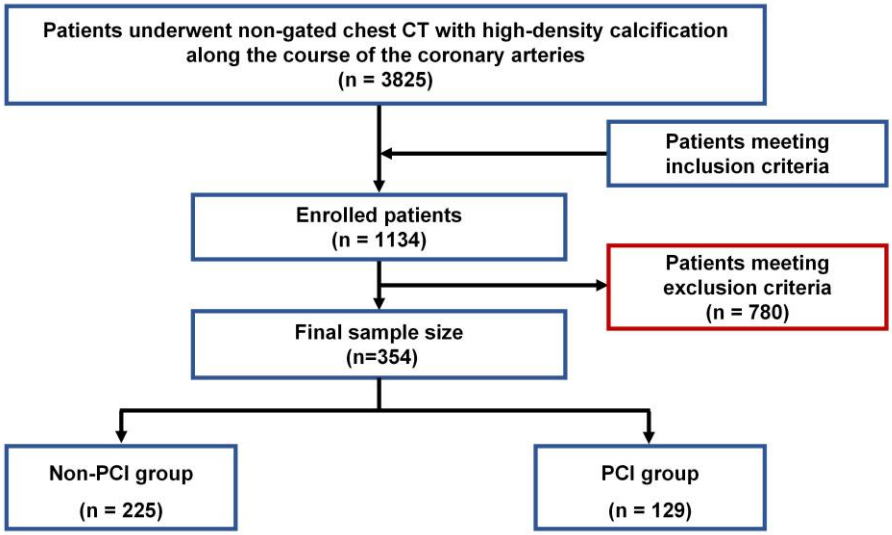


Figure 2. Representative examples of coronary artery calcium segmentation using 3D Slicer. (A) LAD calcium quantification. (B) LCX calcium quantification. (C) RCA calcium quantification.

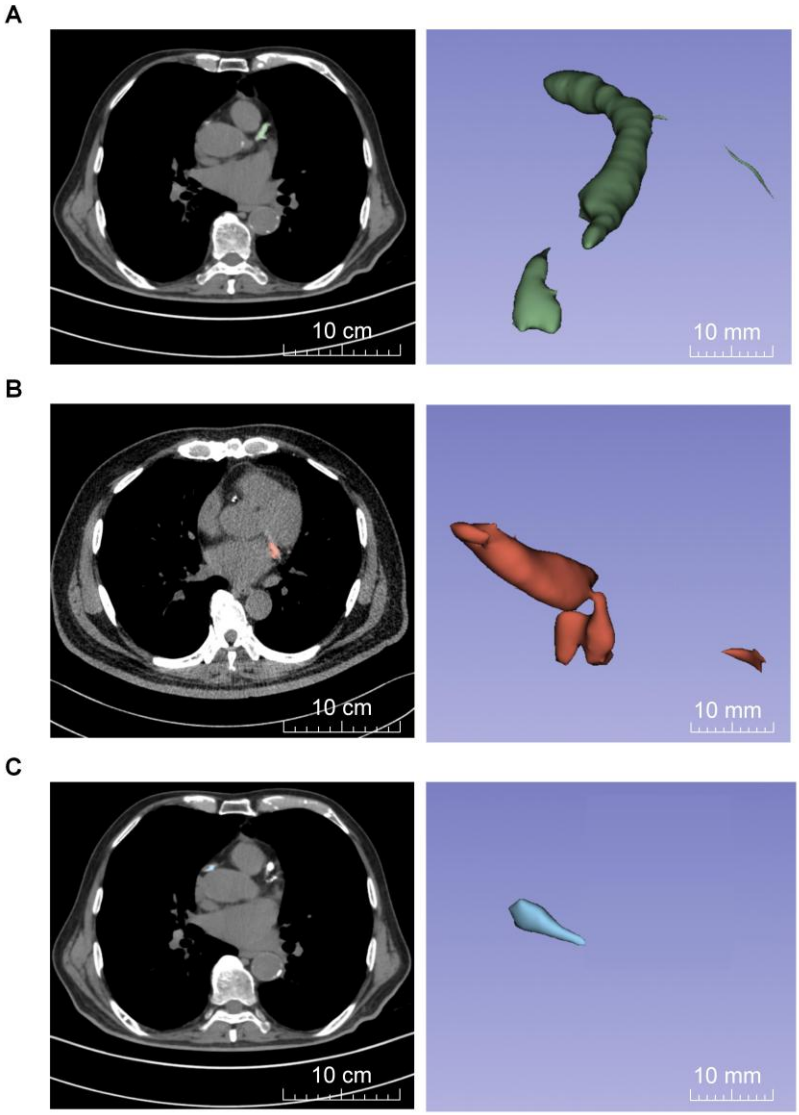


Figure 3. Scatter plots of the correlation between coronary artery calcium volume and angiographic stenosis severity. (A) The Scatter plot of correlation in LAD evaluation. (B) The Scatter plot of correlation in LCX evaluation. (C) The Scatter plot of correlation in RCA evaluation.

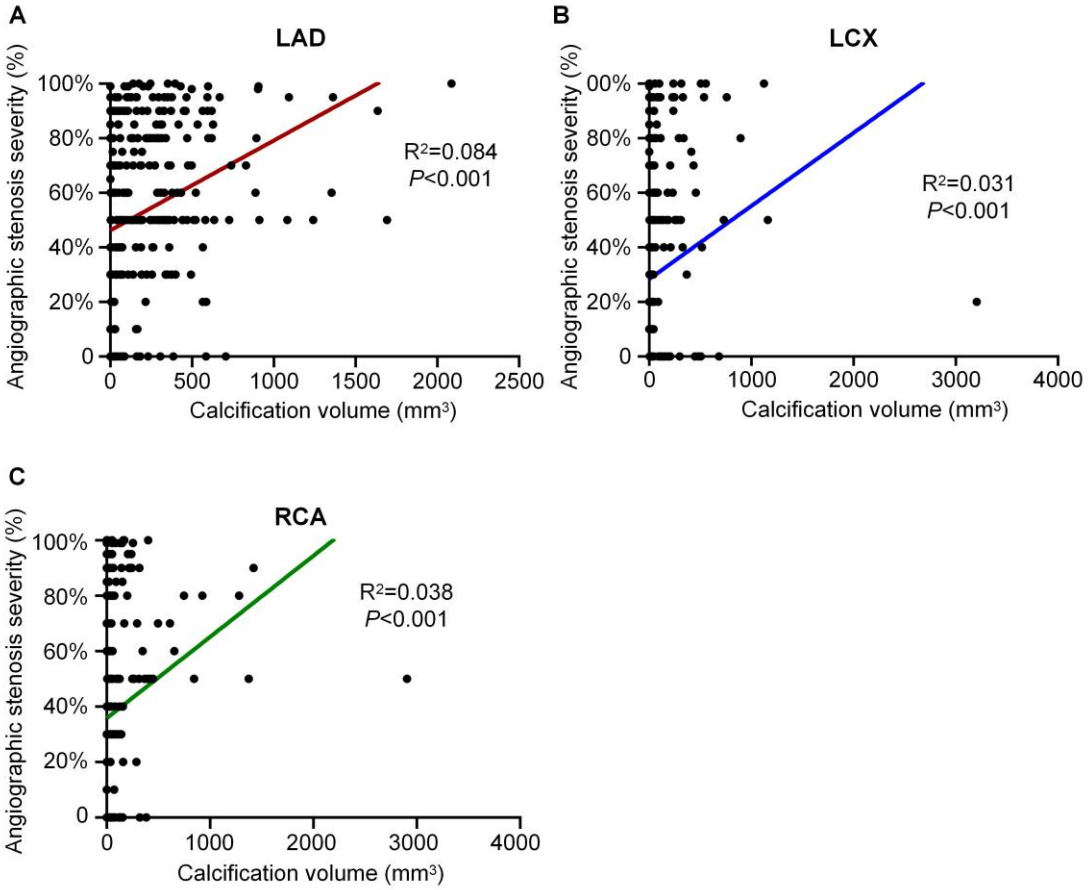


Figure 4. Established artery-specific nomogram for the prediction of PCI. (**A**) Static nomogram for the prediction of LAD. (**B**) Static nomogram for the prediction of LCX. (**C**) Static nomogram for the prediction of RCA.

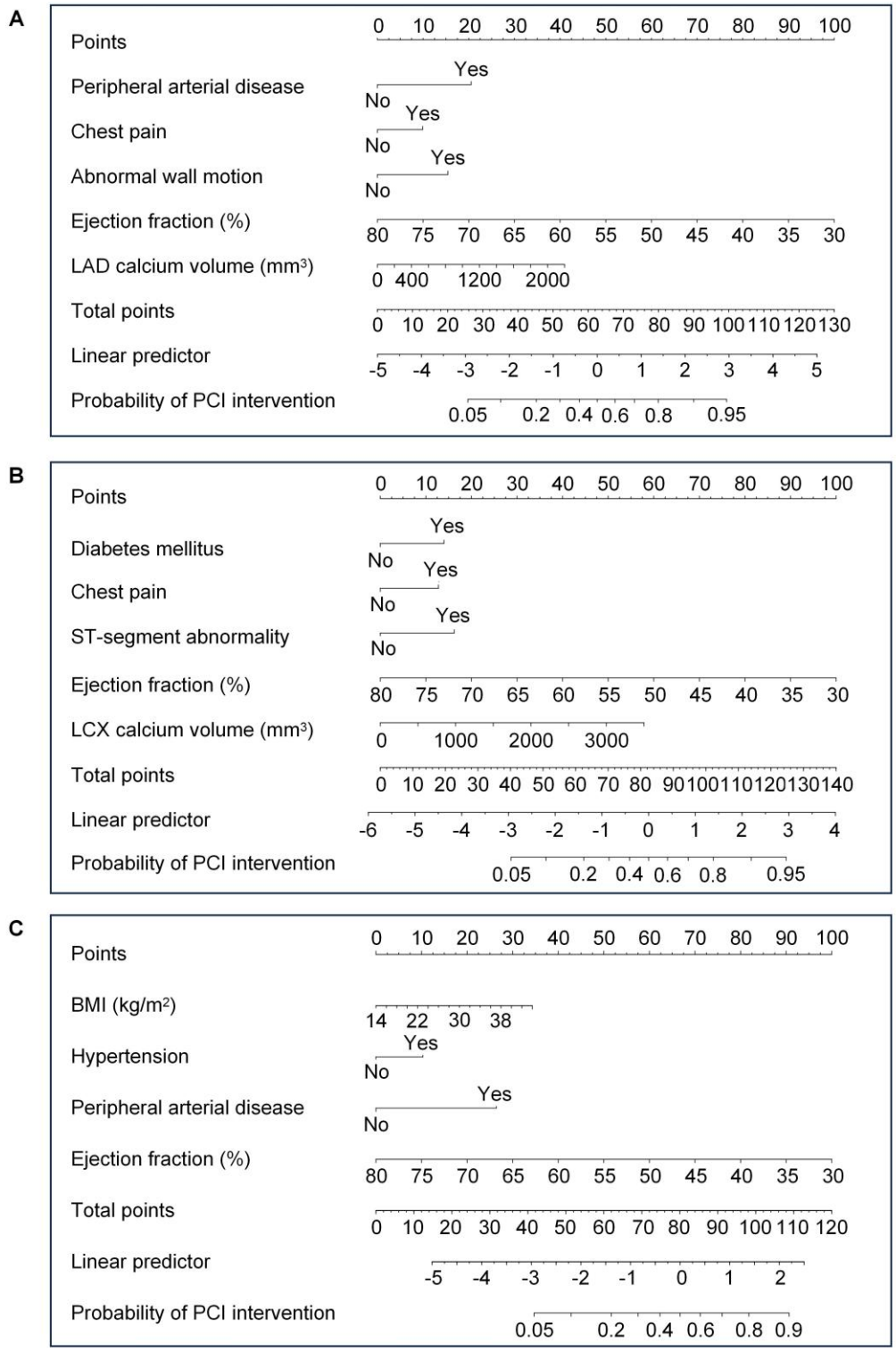
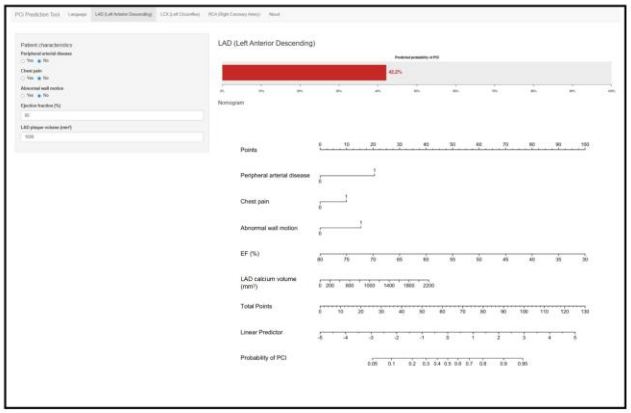


Figure 5. Online dynamic nomogram. (**A**) Accessible at https://zhuyu.shinyapps.io/pci-predictor/, depicting an example for predicting the probability of PCI for a patient (EF=60, LAD calcium volume=1000 mm^3). (**B**) Quick response code of Online dynamic nomogram.

A



B

Figure 6. Prediction efficiency of nomogram prediction. (**A**) ROC curves of coronary intervention models. (B) Calibration curve of prediction of PCI for LAD. (C) Calibration curve of prediction of PCI for LCX. (D) Calibration curve of prediction of PCI for RCA. (E) Decision curve analysis for coronary intervention models.

